Title
Whole-body radiation dosimetry of 2-[F-18]fluoro-A-85380 in human PET imaging studies

Journal
Nuclear Medicine and Biology, 32(8)

ISSN
0969-8051

Authors
Obrzut, S L
Koren, A O
Mandelkern, M A
et al.

Publication Date
2005-11-01

Peer reviewed

Whole-Body Radiation Dosimetry of 2-[^{18}F]Fluoro-A-85380 in Human PET Imaging Studies

Sebastian L. Obrzut[a], Andrei O. Koren[b,c], Mark A. Mandelkern[c,d], Arthur L. Brody[b,c], Carl K. Hoh[a], Edythe D. London[b,c,e,*]

[a]*Department of Radiology, Division of Nuclear Medicine, University of California San Diego, La Jolla, CA 92093, USA*

[b]*Department of Psychiatry and Biobehavioral Sciences, David Geffen School of Medicine, University of California Los Angeles, CA 90024, USA*

[c] *Positron Emission Tomography Center, VA Greater Los Angeles Healthcare System, Los Angeles, CA 90073, USA*

[d]*Department of Physics, University of California Irvine, Irvine, CA 92697, USA*

[e]*Department of Molecular and Medical Pharmacology, David Geffen School of Medicine, University of California Los Angeles, CA 90024, USA*

[*] Corresponding Author. Neuropsychiatric Institute, David Geffen School of Medicine, UCLA, 760 Westwood Plaza, C8-532, Los Angeles, CA 90024, USA. Tel: +1-310-825-0606; Fax: +1-310-825-0812. *Email address*: elondon@mednet.ucla.edu (E.D. London).

Abbreviated title: **2-[^{18}F]Fluoro-A-85380 whole-body dosimetry**

Keywords: 2-[^{18}F]FA; Dosimetry; PET; Nicotinic acetylcholine receptor; Whole body distribution

Abstract

2-[^{18}F]Fluoro-A-85380 (2-[^{18}F]fluoro-3-(2(*S*)-azetidinylmethoxy)pyridine, 2-[^{18}F]FA) is a recently developed PET radioligand for noninvasive imaging of nicotinic acetylcholine receptors. Previous radiation absorbed dose estimates for 2-[^{18}F]FA were limited to evaluation of activity in only several critical organs. Here, we performed 2-[^{18}F]FA radiation dosimetry studies on two healthy human volunteers to obtain data for all MIRDOSE organs. Intravenous injection of 2.9 MBq/kg of 2-[^{18}F]FA was followed by dynamic PET imaging. Regions of interest were placed over images of each organ to generate time–activity curves, from which we computed residence times. Radiation absorbed doses were calculated from the residence times using the MIRDOSE 3.0 program. The urinary bladder wall receives the highest radiation absorbed dose (0.153 mGy/MBq for a 2.4-h voiding interval), followed by the liver (0.0496 mGy/MBq) and the kidneys (0.0470 mGy/MBq). The mean effective dose equivalent is estimated to be 0.0278 mSv/MBq, indicating that radiation dosimetry associated with 2-[^{18}F]FA is within acceptable limits.

1. Introduction

2-[^{18}F]Fluoro-A-85380 (2-[^{18}F]fluoro-3-(2(*S*)-azetidinylmethoxy)pyridine), commonly known as 2-[^{18}F]FA, is a recently developed PET radioligand for imaging studies of nicotinic acetylcholine receptors (nAChRs) in the human brain [1]. Such studies have the potential to elucidate the role of nAChRs in normal brain function as well as in pathological states that are thought to involve these receptors (e.g., Alzheimer's disease, Parkinson's disease, nicotine dependence) [2-8]. *In vivo* imaging of nAChRs also may be helpful in evaluating and establishing dosage regimens for medications targeting or interacting with nAChRs.

[^{11}C]Nicotine was the first PET radioligand used for studying brain nAChRs *in vivo* [9]. It has substantial drawbacks that include a high degree of non-specific binding, strong dependency of cerebral accumulation on cerebral blood flow, and rapid dissociation from the receptor–ligand complex [10-12]. Other ^{11}C-labeled radioligands, such as 3-[(1-[^{11}C]methyl-2(*S/R*)-pyrrolidinyl)methoxy]pyridine and 5-[^{11}C]methyl-A-85380, have been developed for *in vivo* visualization of nAChRs [13-15]. Due to the short half-life of ^{11}C (20 min), however, the use of these probes remains limited. Single photon emission computed tomography (SPECT) with 5-[^{123}I]iodo-A-85380 is an alternative technique for the investigation of nAChRs [16,17], however, spatial resolution and sensitivity of SPECT are generally lower than those of PET. 2-[^{18}F]FA lacks some of the disadvantages of previous nAChR probes [1,18], and exhibits high accumulation in the human thalamus [1], consistent with the known brain regional distribution of nAChRs [19]. Parallel work has been done using another compound of this series, 6-[^{18}F]FA [20].

We undertook this study to determine the maximal dose of 2-[^{18}F]FA that can be safely administered intravenously in human subjects, in order to obtain the highest quality PET images without exceeding accepted radiation dosimetry guidelines. Previous estimates of radiation absorbed dose for 2-[^{18}F]FA were based on the measured activity in only several critical organs and conservative assumptions regarding activity that was not directly measured [1,21]. We performed radiation dosimetry studies on two healthy human volunteers to obtain time-activity data for all target organs, and compared the resulting radiation absorbed dose estimates with previously reported values.

2. Materials and methods

2.1. Subjects

Two healthy men (ages: 23 and 39 years; weights: 68 kg for both subjects) with IQ > 80 (assessed by the Shipley Institute of Living Scale) [22] were enrolled. They did not have any clinical evidence of psychopathology [SCL-90] [23] or psychiatric disorders by DSM-IV criteria [Diagnostic Interview Schedule for DSM-IV (DIS-IV)] [24]. The subjects did not have any prior history of drug abuse, and had not used tobacco within the previous 6 months. The subjects also did not have any medical problems, as assessed by medical history, physical examination, and routine blood screen (including CBC and chemistry panel). The Veterans Affairs Greater Los Angeles Healthcare System (VA GLAHS) Institutional Review Board approved the imaging research protocol and informed consent was obtained from the research subjects before imaging. The radioligand was administered to the human volunteers under VA GLAHS RDRC approval.

2.2. Whole body PET imaging

The radiopharmaceutical 2-[^{18}F]FA was prepared as described previously [18]. Imaging was performed using an Advance Nxi PET scanner (General Electric Medical Systems; Milwaukee, WI) in 2-dimensional mode, with an average transaxial resolution of 6.2 mm full width at half maximum, 4.5 mm plane spacing, and 15.7 cm axial field of view. Calibration of the PET scanner was performed by imaging a phantom containing a known activity of ^{18}F, assayed in a dose calibrator, in order to evaluate tissue activity in units of MBq/ml from region-of-interest (ROI) analysis.

Transmission scans were acquired to correct for tissue attenuation. Subjects received a bolus injection of 2.9 MBq/kg of 2-[^{18}F]FA, followed by four sequential whole-body emission scans, which were initiated at the time of bolus injection and completed at 3 h after injection. Each whole-body scan consisted of seven bed positions, starting above the knees and ending at the top of the head. Each bed position was maintained for a duration of 2:03 min for the first scan, and 5:03 min, 10:03 min, 10:03 min for the second, third, and fourth scan, respectively. After accounting for random and scattered coincidences, decay and dead time, image reconstruction was performed using attenuation-corrected filtered back projection.

At predetermined intervals, starting immediately after the 2-[^{18}F]FA administration to 1 h post-injection, the participants were asked whether they felt effects of the injected radioligand. Heart rate, blood pressure, respiratory rate, and ECG parameters were monitored at predetermined intervals throughout the 3-h scanning period.

2.3. Radiation absorbed dose estimates

Reconstructed PET images were used to identify and evaluate the activity in each source organ listed in Table 1. Regions of interest (ROI) were manually drawn within the boundaries of organs in adjacent transaxial slices at each time point. Organs demonstrating low activity on the transverse projection were first identified on coronal or sagittal whole body images, which provide greater anatomic detail, and then localized on transverse planes using triangulation to delineate their boundaries. For each time point of a dynamic scan, data from each ROI (counts/pixel) were corrected for time of acquisition and tomograph efficiency using the phantom data. These results were converted to units of MBq/ml. The specific measurement time assigned to each organ was the estimated midpoint of the time that the organ was in the scanner field of view during each of the sequential whole-body scans. Mean activity per unit volume was calculated from all ROIs for each organ, assuming a uniform distribution of activity within the organ. This value was divided by the organ tissue density, multiplied by the standard reference organ weight [25], and divided by the administered activity in order to estimate the fraction of administered activity in the given organ at a given time point. The administered activity was first adjusted by multiplying it by the ratio of the actual patient weight and the standard patient weight of 70 kg. We assumed the lung tissue density to be 0.33 g/ml and the tissue density of other organs to be 1.0 g/ml [26].

For all organs except the bladder, residence times (in hours) were determined using trapezoidal integration of the decay-corrected time-activity curve from zero time to the time of the last PET scan. Thus, four time points were used to construct each time-activity curve. Residence time for a source organ was defined as the area under the decay-

corrected time-activity curve, divided by the amount of activity administered. Beyond the last time point, we assumed physical decay of the ^{18}F label without biological clearance. The residence time of the urinary bladder content was calculated by applying the dynamic bladder model according to Cloutier [27], which is included in the MIRDOSE 3.0 program. For calculations, voiding intervals of 2.4 h and 1 h, as defined in the MIRDOSE 3.0 program, were assumed. Values of biological half-time of 4 h and clearance of 91% via the urinary pathway, obtained from previously published results [1], were used in the calculations of bladder residence times. The radiation absorbed dose was calculated by multiplying the residence-time values by the appropriate S values, defined by the Medical Internal Radiation Dose (MIRD) system [28]. To perform the final radiation-absorbed-dose calculations, the residence times were transferred to the MIRDOSE program (Version 3.0, ORISE, Oak Ridge, TN) [29], which yielded the single-organ radiation absorbed doses as well as the effective dose equivalent.

3. Results

On early PET whole body images, 10 min after injection of 2-[^{18}F]FA, intense activity was seen in the liver, kidneys, and intestines; and low activity was observed in the lungs, brain, and heart wall. On later images, 2-3 h after injection of the radioligand, activity was markedly retained within the urinary bladder, liver, kidneys, bone marrow, brain, and the spleen. A representative coronal whole-body PET image, obtained at 118 min after 2-[^{18}F]FA administration, is shown in Figure 1.

Place Figure 1 approximately here.

The residence times for each measured source organ, except the urinary bladder, are shown in Table 1. The residence time for the urinary bladder, calculated by applying the

dynamic bladder model [27] is 0.31 h for the 2.4-h voiding interval and 0.14 h for the 1-h voiding interval. The mean radiation absorbed dose and standard-deviation estimates for 2-[^{18}F]FA, assuming the 2.4-h voiding interval, are shown in Table 2. The urinary bladder is the most dosimetry-critical organ. The bladder wall receives a mean radiation absorbed dose of 0.071 mGy/MBq for the 1-h voiding interval, and 0.153 mGy/MBq for the 2.4-h voiding interval. Other organs that receive relatively high radiation absorbed doses are the liver (0.0496 mGy/MBq), kidneys (0.0470 mGy/MBq), pancreas (0.0250 mGy/MBq), spleen (0.0247 mGy/MBq), gallbladder wall (0.0228 mGy/MBq), and adrenal glands (0.0212 mGy/MBq). The mean effective dose equivalent is 0.0278 mSv/MBq.

No adverse events were observed in either of the research participants after administration of 2-[^{18}F]FA. There was no significant rise in body temperature, indicating that the 2-[^{18}F]FA solution was apyrogenic. In addition, 2-[^{18}F]FA had no observable effect on blood pressure, and ECG recordings remained normal after the radiotracer injection.

Place Tables 1 and 2 approximately here.

4. Discussion

This study was conducted to estimate the radiation absorbed dose resulting from the intravenous injection of 2-[^{18}F]FA in order to assess the radiation risk associated with PET imaging with this radioligand. 2-[^{18}F]FA radiation-dosimetry calculations indicate that the urinary bladder is the critical organ, receiving the highest radiation absorbed dose. Since the voiding interval affects the radiation absorbed dose, we considered 2.4 h and 1 h bladder voiding intervals, as done previously [1], to estimate the impact of voiding on radiation exposure. For the 2.4-h interval, the urinary bladder wall receives a mean

radiation absorbed dose of 0.153 mGy/MBq (0.566 rad/mCi). For the 1-h voiding interval, on the other hand, the mean dose absorbed by the urinary bladder wall is 0.071 mGy/MBq (0.262 rad/mCi).

According to the Code of Federal Regulations (CFR), in research subjects, the single dose limit to blood-forming organs, the gonads, and the whole body is 3 rem, and the annual and total dose commitment limit is 5 rem [30]. Furthermore, the single-dose limit for urinary bladder wall is 5 rem, and the annual and total dose-commitment limit is 15 rem. Therefore, to comply with the CFR limits, the maximum activity that may be administered in a single 2-[^{18}F]FA PET study, with a 2.4 h voiding interval, is 327.87 MBq (8.86 mCi). At this level, the doses to sensitive organs, such as the testes and bone marrow, are well below the 3 rem limit set forth by the CFR. The maximum activity that may be administered annually to a person in 2-[^{18}F]FA PET studies, with a 2.4-h voiding interval, is 983.61 MBq (26.58 mCi).

In research subjects who could void every hour, the bladder would remain the critical organ, but the bladder radiation absorbed dose would be reduced to 0.071 mGy/MBq (0.262 rad/mCi). More frequent voiding would raise the allowable 2-[^{18}F]FA amount for a single imaging study to 705.22 MBq (19.06 mCi). Furthermore, the maximum activity that could be administered annually with a 1 h voiding interval would be 2115.66 MBq (57.18 mCi). These estimates demonstrate that more frequent patient voiding would allow the administration of greater amounts of 2-[^{18}F]FA, resulting in improved counting statistics and, accordingly, higher image quality.

It should be noted that in addition to the simplifications inherent in the MIRD phantom model, several other assumptions were made in analyzing our 2-[^{18}F]FA imaging

data. The radioactivity distribution was assumed to be homogeneous throughout each organ. During dynamic PET imaging, the radioligand clearance occurs by both biological elimination and physical decay, however, the clearance was assumed to have only physical decay component after the final imaging time point. This conservative assumption should result in an overestimation of the calculated radiation absorbed doses. Furthermore, residence times were determined using trapezoidal integration of time-activity data for all organs except the bladder. Finally, this study did not evaluate the radiation absorbed dose to the ovaries and uterus, since only male research subjects participated in our study. Nonetheless, Kimes et al., who included at least one female subject in their study did not report remarkable radioactivity in the uterus or the ovaries [1].

Our report extends previous work to estimate radiation absorbed dose resulting from administration of 2-[^{18}F]FA [1,21]. In one of the previous reports, residence time for the urinary bladder was determined from excreted radioactivity in 6 subjects, and residence times for seven organs were determined from data obtained in 2 or 3 subjects with three whole body scans for each [1]. That report provided the absorbed dose equivalent for the urinary bladder wall, kidneys and liver, and a combined value for all other organs. In this study, we report radiation-dosimetry estimates, which were obtained using activity data for 20 source organs (Table 1). Our estimated radiation absorbed doses for the testes, thyroid gland, lungs, and heart wall exceed those reported in one of the two previous reports on this topic [21]. However, the prior study, which included 3 subjects, did not evaluate the residence times of these organs and did not provide an account of the contribution of the actual activity of these organs to their radiation absorbed doses. If not considered, these factors would result in an underestimation of radiation absorbed doses.

Our data indicate that the organ with the greatest mean residence time is skeletal muscle (0.811 h). The reason for this phenomenon is not clear although we note that A-85380 and its iodo derivative have low affinity for the muscle-type nicotinic receptor (19 and 140 μM, respectively) [31].

MIRDOSE 3.0 calculations reveal that muscle radioactivity contributes to the doses absorbed by the thyroid gland (22%), spleen (10%), lungs (10%), liver (4%), and brain (3%). The estimated radiation absorbed doses for these organs also exceed those reported previously [21]. However, since the prior study did not evaluate the residence time of muscle, it probably did not account for the contribution of muscle radioactivity to the radiation absorbed doses for these organs. Again, this would result in an underestimation of radiation absorbed doses. Finally, Kimes et al. estimated the mean effective dose equivalent to be less than 0.045 mSv/MBq [1]. This value exceeds our estimate by a factor of nearly two, possibly because Kimes et al. assumed the residence times for most organs to be equal to the residence time of the liver [1], resulting in an overestimation of radiation absorbed doses.

5. Conclusion

2-[^{18}F]FA is a safe PET radioligand with pharmacokinetic properties suitable for the imaging of central nAChRs. The organ and total-body radiation absorbed doses received in a 2-[^{18}F]FA PET imaging study are comparable to those associated with other widely used clinical nuclear medicine procedures [e.g., 32] and are below the CFR limits established for research subjects. This analysis shows that the radiation dosimetry of 2-[^{18}F]FA is favorable for further use of this imaging agent for human PET studies.

References

[1] Kimes AS, Horti AG, London ED, Chefer SI, Contoreggi C, Ernst M, Friello P, Koren AO, Kurian V, Matochik JA, Pavlova O, Vaupel DB, Mukhin AG. 2-[^{18}F]F-A-85380: PET imaging of brain nicotinic acetylcholine receptors and whole body distribution in humans. FASEB J 2003:17:1331-1333.

[2] Court JA, Martin-Ruiz C, Graham A, Perry E. Nicotinic receptors in human brain: topography and pathology. J Chem Neuroanat 2000:20:281-298

[3] Breese CR, Marks MJ, Logel J, Adams CE, Sullivan B, Collins AC, Leonard S. Effect of smoking history on [^{3}H]nicotine binding in human postmortem brain. J Pharmacol Exp Ther 1997:282:7-13.

[4] Perry DC, Dávila-García MI, Stockmeier CA, Kellar KJ. Increased nicotinic receptors in brains from smokers: Membrane binding and autoradiography studies. J Pharmacol Exp Ther 1999:289:1545-1552.

[5] Rinne JO, Myllykyla T, Lonnberg P, Marjamaki P. A postmortem study of brain nicotinic receptors in Parkinson's and Alzheimer's disease. Brain Res 1991:547:167-170.

[6] Warpman U, Nordberg A. Epibatidine and ABT 418 reveal selective losses of alpha 4 beta 2 nicotinic receptors in Alzheimer brains. Neuro Report 1995:6:2419-2423.

[7] Newhouse PA, Potter A, Levin ED. Nicotinic system involvement in Alzheimer's and Parkinson's diseases. Implications for therapeutics. Drugs Aging 1997:11:206-228.

[8] Nordberg A, Winblad B. Reduced number of [^{3}H]nicotine and [^{3}H]acetylcholine binding sites in the frontal cortex of Alzheimer brains. Neurosci Lett 1986:72:115-119.

[9] Muzic Jr RF, Berridge MS, Friedland RP, Zhu N, Nelson AD. PET quantification of specific binding of carbon-11-nicotine in human brain. J Nucl Med 1998:39:2048-2054.

[10] Kassiou M, Ravert HT, Mathews WB, Musachio JL, London ED, Dannals RF. Synthesis of 3-[(1-[11C]methyl-2(S)-pyrrolidinyl)methoxy]pyridine and 3-[1-[11C]methyl-2-(R)-pyrrolidinyl)-methoxy]pyridine: Radioligands for in vivo studies of neuronal nicotinic acetylcholine receptors. J Labelled Comp Radiopharm 1997:39:425-431.

[11] Kassiou M, Scheffel UA, Ravert HT, Mathews WB, Musachio JL, London ED, Dannals RF. Pharmacological evaluation of [11C]A-84543: an enantio-selective ligand for in vivo studies of neuronal nicotinic acetylcholine receptors. Life Sci 1998:63:PL13-8

[12] Iida Y, Ogawa M, Ueda M, Tominaga A, Kawashima H, Magata Y, Nishiyama S, Tsukada H, Mukai T, Saji H. Evaluation of 5-(11)C-methyl-A-85380 as an imaging agent for PET investigations of brain nicotinic acetylcholine receptors. J Nucl Med 2004:45:878-884.

[13] Lundqvist H, Nordberg A, Hartvig P, Langstrom B. (S)-(-)-[11C]nicotine binding assessed by PET: a dual tracer model evaluated in the rhesus monkey brain. Alzheimer Dis Assoc Disord 1998:12:238-246.

[14] Sihver W, Nordberg A, Langstrom B, Mukhin AG, Koren AO, Kimes AS, London ED. Development of ligands for in vivo imaging of cerebral nicotinic receptors. Behav Brain Res 2000:113:143-157.

[15] Maziere M, Delforge J. PET imaging of [^{11}C]nicotine: Historical aspects in brain imaging of nicotine and tobacco smoking. (Domino, E. F., ed), NPP Books, Ann Arbor; 1995, p. 13-28.

[16] Fujita M, Seibyl JP, Vaupel DB, Tamagnan G, Early M, Zoghbi SS, Baldwin RM, Horti AG, Koren AO, Mukhin AG, Khan S, Bozkurt A, Kimes AS, London ED, Innis RB. Whole-body biodistribution, radiation absorbed dose, and brain SPET imaging with [^{123}I]5-I-A-85380 in healthy human subjects. Eur J Nucl Med 2002:29:183-190.

[17] Mamede M, Ishizu K, Ueda M, Mukai T, Iida Y, Fukuyama H, Saga T, Saji H. Quantification of human nicotinic acetylcholine receptors with ^{123}I-5IA SPECT. J Nucl Med 2004:45:1458-1470.

[18] Horti AG, Scheffel U, Koren AO, Ravert HT, Mathews WB, Musachio JL, Finley PA, London ED, Dannals RF. 2-[^{18}F]Fluoro-A-85380, an in vivo tracer for the nicotinic acetylcholine receptors. Nucl Med Biol 1998:25:599-603.

[19] London ED, Waller SB, Wamsley JK. Autoradiographic localization of [^{3}H]-nicotine binding sites in the rat brain. Neurosci Lett 1985:53:179-184.

[20] Ding YS, Fowler JS, Logan J, Wang GJ, Telang F, Garza V, Biegon A, Pareto D, Rooney W, Shea C, Alexoff D, Volkow ND, Vocci F. 6-[18F]Fluoro-A-85380, a new PET tracer for the nicotinic acetylcholine receptor: studies in the human brain and in vivo demonstration of specific binding in white matter. Synapse 2004:53:184-189.

[21] Bottlaender M, Valette H, Roumenov D, Dolle F, Coulon C, Ottaviani M, Hinnen F, Ricard M. Biodistribution and radiation dosimetry of ^{18}F-fluoro-A-85380 in healthy volunteers. J Nucl Med 2003:44:596-601.

[22] Zachary RA. Shipley Institute of Living Scale. Los Angeles, CA: Western Psychological Services, 1986.

[23] Derogatis LR, Lipman RS, Covi L. SCL-90: an outpatient psychiatric rating scale--preliminary report. Psychopharmacol Bull 1973:9:13-28.

[24] Robins L, Cottler L, Bucholz K, Compton W. Diagnostic Interview Schedule for DSM-IV. St. Louis, MO: Washington University, 1995.

[25] Cristy M, Eckerman K. Specific absorbed fractions of energy at various ages from internal photon sources, I–VII. Oak Ridge, TN: Oak Ridge National Laboratory, ORNL/TM-8381 V1–V7, 1987.

[26] Rhodes CG, Wollmer P, Fazio F, Jones T. Quantitative measurement of regional extravascular lung density using positron emission and transmission tomography. J Comput Assist Tomogr 1981:5:783-791.

[27] Cloutier RJ, Smith SA, Watson EE, Snyder WS, Warner GG. Dose to the fetus from radionuclides in the bladder. Health Phys 1973:25:147-161.

[28] Loevinger R, Budinger T, Watson E. MIRD Primer for Absorbed Dose Calculations. Reston, VA: Society of Nuclear Medicine, 1988.

[29] Stabin MG. MIRDOSE: personal computer software for internal dose assessment in nuclear medicine. J Nucl Med 1996:37:538-546.

[30] Code of Federal Reguations. Title 21, Part 361.1, 4-1 Edition, 2004.

[31] Mukhin AG, Gündisch D, Horti AG, Koren AO, Tamagan G, Kimes AS, Chambers J, Vaupel DB, King SL, Picciotto MR, Innis RB, London ED. 5-Iodo-A-85380, an α4β2 subtype-selective ligand for nicotinic acetylcholine receptors. Mol Pharmacol 2000: 57:642-649.

[32] Deloar HM, Fujiwara T, Shidahara M, Nakamura T, Watabe H, Narita Y, Itoh M, Miyake M, Watanuki S. Estimation of absorbed dose for 2-[^{18}F]fluoro-2-deoxy-D-glucose using whole-body positron emission tomography and magnetic resonance imaging. Eur J Nucl Med 1998:25:565-574.

Table 1. Residence Time (Hours) of 2-[^{18}F]FA for Measured Source Organs

Organ	Subject 1	Subject 2	Mean	SD
Adrenals	1.40E-03	8.00E-04	1.10E-03	4.24E-04
Liver	4.60E-01	2.63E-01	3.62E-01	1.39E-01
Brain	1.03E-01	8.31E-02	9.31E-02	1.41E-02
Lungs	8.78E-02	8.17E-02	8.48E-02	4.31E-03
Breasts	1.08E-02	9.10E-03	9.95E-03	1.20E-03
Muscle	9.10E-01	7.12E-01	8.11E-01	1.40E-01
Gall Bladder	7.30E-03	4.40E-03	5.85E-03	2.05E-03
Pancreas	1.26E-02	3.80E-03	8.20E-03	6.22E-03
Lower Large Intestine	6.20E-03	5.20E-03	5.70E-03	7.07E-04
Red Marrow	1.34E-01	5.72E-02	9.56E-02	5.43E-02
Small Intestine	2.43E-02	4.46E-02	3.45E-02	1.44E-02
Cortical Bone	8.39E-02	8.86E-02	8.63E-02	3.32E-03
Stomach	1.63E-02	1.56E-02	1.60E-02	4.95E-04
Trabecular Bone	2.70E-02	3.67E-02	3.19E-02	6.86E-03
Upper Large Intestine	2.36E-02	1.66E-02	2.01E-02	4.95E-03
Spleen	2.11E-02	1.44E-02	1.78E-02	4.74E-03
Heart Wall	1.90E-02	1.73E-02	1.82E-02	1.20E-03
Testes	2.20E-03	1.80E-03	2.00E-03	2.83E-04
Kidneys	6.67E-02	6.02E-02	6.35E-02	4.60E-03
Thyroid	1.00E-03	1.10E-03	1.05E-03	7.07E-05

Table 2. Radiation Absorbed Dose Estimates for 2-[^{18}F]FA (mGy/MBq)

Target Organ	Mean	SD
Adrenals	2.12E-02	6.86E-03
Bone Surfaces	1.35E-02	2.40E-03
Brain	1.73E-02	2.62E-03
Breasts	8.49E-03	1.29E-03
Gallbladder Wall	2.28E-02	7.07E-03
Heart Wall	1.66E-02	2.12E-03
Kidneys	4.70E-02	4.74E-03
Liver	4.96E-02	1.82E-02
Lower Large Intestine Wall	1.25E-02	1.13E-03
Lungs	1.99E-02	2.05E-03
Muscle	9.85E-03	1.63E-03
Pancreas	2.50E-02	1.39E-02
Red Marrow	1.41E-02	4.60E-03
Skin	3.18E-03	5.30E-04
Small Intestine	1.43E-02	1.56E-03
Spleen	2.47E-02	6.15E-03
Stomach	1.24E-02	1.56E-03
Testes	1.44E-02	1.70E-03
Thymus	4.69E-03	8.63E-04
Thyroid	1.23E-02	7.07E-05
Upper Large Intestine Wall	1.60E-02	2.90E-03
Urinary Bladder Wall	1.53E-01	7.07E-04
Total Body	9.66E-03	1.76E-03
Effective Dose Equivalent	2.78E-02	4.03E-03
Effective Dose (mSv/MBq)	2.37E-02	2.90E-03

Figure caption

Fig. 1. Representative coronal whole-body PET image obtained at 118 min after injection of 197 MBq of 2-[^{18}F]FA. The scan shows increased tracer activity in the urinary bladder, liver, kidneys, bone marrow, brain and spleen. The whole body PET scan was completed in 1:10:20 h (10:03 min per bed position, 7 positions).

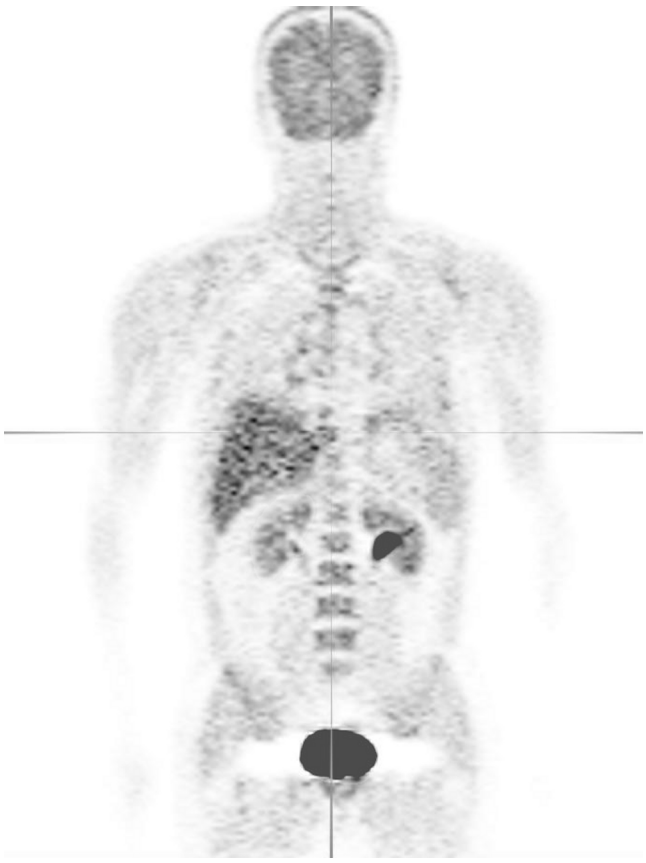

Figure 1.